Flow Measurement and Instrumentation ▮ (▮▮▮▮) ▮▮▮–▮▮▮

Contents lists available at ScienceDirect

Flow Measurement and Instrumentation

journal homepage: www.elsevier.com/locate/flowmeasinst

Sensorless measurement of pulsatile flow rate using a disturbance force observer in a magnetically levitated centrifugal blood pump during ventricular assistance

Chi Nan Pai [a], Tadahiko Shinshi [b,*], Akira Shimokohbe [b]

[a] Interdisciplinary Graduate School of Science and Engineering, Tokyo Institute of Technology, R2-38, 4259 Nagatsuta, Midori-ku, Yokohama 226-8503, Japan

[b] Precision and Intelligence Laboratory, Tokyo Institute of Technology, R2-38, 4259 Nagatsuta, Midori-ku, Yokohama 226-8503, Japan

ARTICLE INFO

Article history:
Received 27 May 2009
Received in revised form
17 September 2009
Accepted 2 November 2009

Keywords:
Maglev centrifugal pump
Ventricular assist device
Sensorless measurement
Radial thrust
Pulsatile flow

ABSTRACT

Implantable rotary pumps have been developed and used to assist the impaired heart ventricle because of lack of heart donors for transplant. Pulsatile flow rate measurement is important for controlling the flow rate of these rotary pumps. Conventional flow meters are not particularly compact; while the reliability and durability of small flow meters made using micro-electro-mechanical system technology is still uncertain. Several groups have proposed estimating flow rate using the motor power of the centrifugal blood pump (CBP), but none have succeeded in accurately estimating pulsatile flow rate.

We have developed an implantable CBP, employing a two degrees-of-freedom radial controlled magnetic bearing (MB) to support the impeller without contact, which decreases the damage to blood cells and increases the durability of the device. The radial thrust acting on the impeller depends on the rotational speed of the impeller and the contractility of the heart ventricle. In this study we present a method to measure pulsatile flow rate during ventricular assistance, using the radial thrust estimated by the radial disturbance force observer of the MB of the CBP.

The variable parameters of the dynamic model of the maglev impeller were identified for different flow conditions, assuming the density and viscosity of the water to be constant. The design of the disturbance force observers was based on the linear models obtained for a given rotational speeds.

Under non-pulsatile conditions, the relationship between the measured flow rate and the estimated radial thrust was experimentally obtained. Using this relationship, under pulsatile conditions, a high correlation ($r > 0.94$) between the measured and estimated flow rate was obtained, with a maximum estimation error of 0.3 L/min (15%) for average pulsatile flow rate and 0.5 L/min (7%) for the amplitude of pulsatile flow rate. Also, by observing the amplitude of the pulsatile flow rate, the backflow could be ascertained.

1. Introduction

Implantable ventricular assist devices (VADs) have been developed and used to solve the problem of lack of donors for heart transplants. The implantable VAD is connected to the left ventricle of the impaired heart in order to assist its pumping function. Patients with an implantable VAD have shown good clinical results and improvements in the left ventricle function and in the quality of life [1–4].

In order to be implantable, a VAD should be compact and biocompatible, should cause little damage to blood cells and no blood clot formation, and should have high reliability and high durability. Rotary pumps have advantages over pulsatile pumps in that they are more compact and more durable. Therefore, they are a good choice for implantable devices. Fig. 1(a) shows a schematic of an implantable ventricular assist system using a rotary pump.

To control the flow rates of rotary pumps, measurement of the flow rate is required. Conventional flow meters are not compact, and require more space in the body. Another option for flow rate measurement is the development of small flow meters based on micro-electro-mechanical system (MEMS) technology. However, the durability and reliability of these devices remains uncertain.

Furthermore, when a rotary pump is attached to the heart ventricle and the aorta, the pump flow is influenced by the cardiovascular system. Thus, the contractility of the natural heart causes the flow to be pulsatile and pulsatile flow has an average and amplitude of the flow rate.

In order to measure flow rate without having to implant a conventional flow meter, several groups have proposed flow rate estimation methods based on the motor power and rotational speed [5–8] of a centrifugal blood pump (CBP). However, none of these proposed methods succeeded in accurately estimating pulsatile flow rate.

* Corresponding author. Tel.: +81 45 924 5095; fax: +81 45 924 5046.
E-mail address: shinshi@pi.titech.ac.jp (T. Shinshi).

0955-5986/$ – see front matter © 2009 Elsevier Ltd. All rights reserved.
doi:10.1016/j.flowmeasinst.2009.11.003

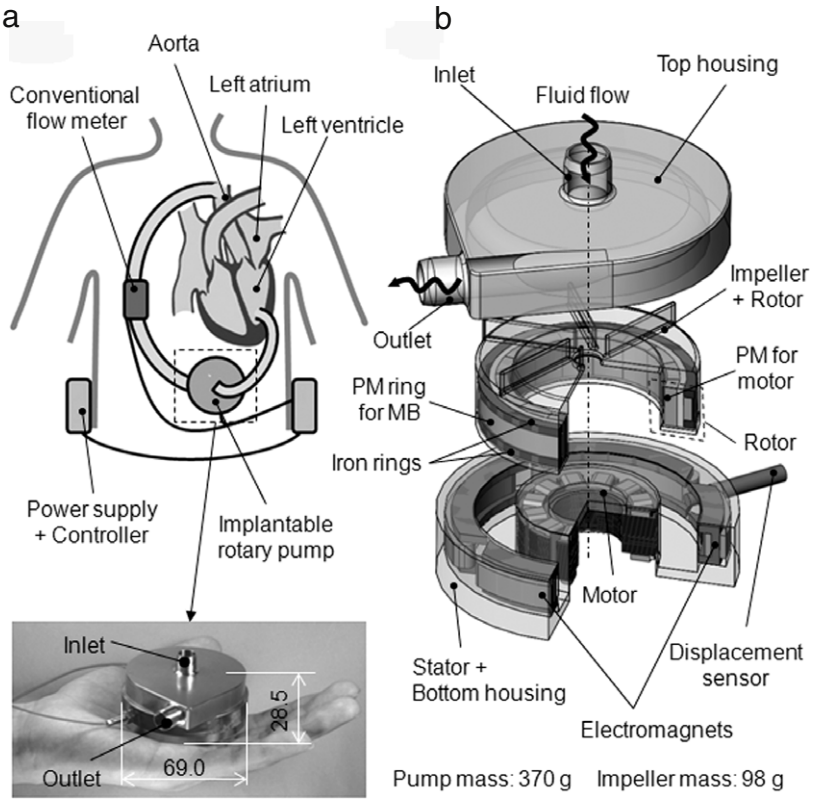

Fig. 1. (a) Ventricular assist system and photograph of an implantable maglev CBP, and (b) configuration of the implantable maglev CBP.

Ayre et al. and Tsukiya et al. presented methods for estimating the average flow rate [5,6] for CBPs with non-contact bearings. Although their methods gave low errors for estimating the average flow rate (6% and 12% respectively), the amplitude of the pulsatile flow rate was not estimated.

Tsukiya et al. and Ogawa et al. proposed methods for estimating pulsatile flow rate in CBPs with contact bearings [7,8]. Although the amplitude of the pulsatile flow rate was estimated, their errors were not given and the estimated average flow rates showed errors of up to 17% and 21%, respectively, during chronic animal experiments.

Other groups have proposed using the displacement of the magnetically levitated (maglev) impeller in a CBP to estimate the flow rate [9,10]. The displacement of the maglev impeller is induced by the radial thrust, which is related to the rotational speed of the impeller and the pulsatile condition of the heart ventricle. So, understanding the radial thrust acting on the maglev impeller in real time provides a means of estimating the pulsatile flow rate.

Our group has developed a two degrees-of-freedom radial controlled maglev CBP to be used as an implantable VAD [11]. This maglev CBP has a radial magnetic bearing (MB) to levitate the impeller without mechanical contact, increasing the durability of the pump and also decreasing the damage to the blood cells. Using the radial MB of this CBP, we also developed a radial disturbance force observer to estimate the radial thrust acting on the maglev impeller [12]. The designed disturbance force observer has high estimation accuracy and a bandwidth of 45 Hz, sufficient for estimating the radial thrust under pulsatile flow conditions. The purpose of this study is to use the radial thrust estimated using the radial disturbance force observer to measure the pump pulsatile flow rate.

2. Flow rate estimation process

2.1. Principle

Rotary pumps convert electrical power into hydraulic power, which is a function of head pressure and flow rate. A CBP usually has a flat pump characteristic curve (HQ curve), which results in a small variation of head pressure for a wide range of flow rates. By assuming the head pressure to be either constant or a function of flow rate, a direct relationship between the motor power, flow rate and rotational speed can be obtained.

Since several groups have examined this approach but none has shown good accuracy in estimating pulsatile flow rate [5–8], we propose another approach using the relationship between the radial thrust and the flow rate.

According to Stepanoff [13], the radial thrust (F_{rt}) is a function of head pressure (H) and flow rate (Q), in the form shown in Eq. (1).

$$F_{rt} = KHQ. \quad (1)$$

K is a constant that depends on pump parameters, such as the impeller diameter, the vane height, etc.

The head pressure was assumed to be constant in forming the relationship between the flow rate and the radial thrust, because of the flat HQ curve of the CBP. The proposed flow rate estimation process involves identification of the relationship between the radial thrust and the flow rate, estimation of radial thrust using the disturbance force observer, and using the radial thrust with the identified relationship to estimate the pulsatile flow rate. The entire flow rate estimation process is summarized in Fig. 2.

2.2. Radial disturbance force observer

Flow conditions, such as the working fluid, the rotational speed, and the flow resistance, influence the dynamic characteristics of a

Please cite this article in press as: Pai CN, et al. Sensorless measurement of pulsatile flow rate using a disturbance force observer in a magnetically levitated centrifugal blood pump during ventricular assistance. Flow Measurement and Instrumentation (2009), doi:10.1016/j.flowmeasinst.2009.11.003

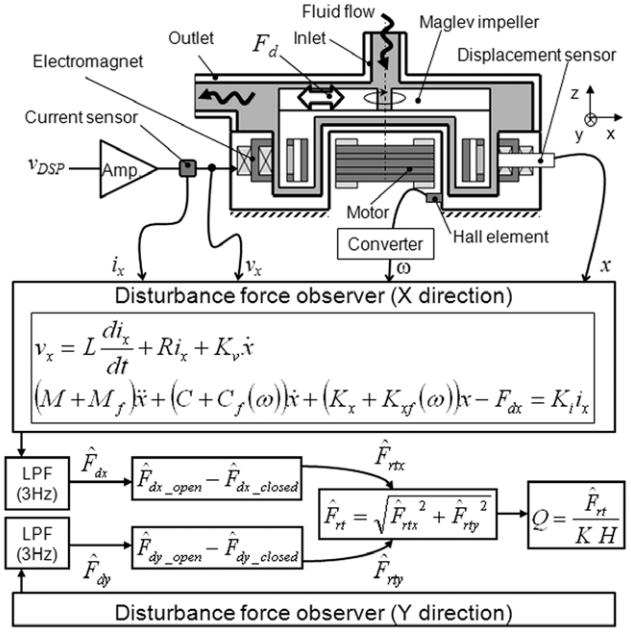

Fig. 2. Flow rate estimation process using a disturbance force observer.

maglev impeller [14]. In order to evaluate the dynamic characteristics of the radial motion of the impeller and to design the disturbance observer, a dynamic model of the maglev system was constructed, taking into consideration the effects of the fluid, the rotational speed (ω) and the flow resistance, and variable model parameters, such as additional mass (M_f), additional damping (C_f) and additional stiffness (K_{xf}), were identified experimentally [12].

According to Fung and Kim, blood behaves as a Newtonian fluid at high shear rates ($>100\ s^{-1}$) [15,16]. The shear rate in our maglev CBP is higher than $1.8 \times 10^4\ s^{-1}$ at 1700 rpm. Therefore, the blood will behave as a Newtonian fluid, similar to water.

When blood, which has a dynamic viscosity (μ) of 2.7×10^{-3} Ns/m^2 [15] and a density (ρ) of 1060 Kg/m^3 [17] at 37 °C, is used as a working fluid, the Reynolds number [18], as in Eq. (2), is 2.9×10^4 at 1700 rpm and 37 °C. When water, which has a dynamic viscosity of 1.002×10^{-3} Ns/m^2 and a density of 998.2 Kg/m^3 at 20 °C, is used, $Re = 7.3 \times 10^4$ at 1700 rpm and 20 °C. According to Sinnott, the pump system is fully turbulent for values of Reynolds number above 10 000 [18]. Therefore, the flows in our pump when using blood or water as the working fluid are turbulent.

$$Re = \frac{\rho\omega d^2}{\mu} \tag{2}$$

where d is the diameter of the impeller.

Based on these results, for experimental simplicity, water was used instead of blood. The density and viscosity of water were assumed to be constant, and the variable model parameters were identified for different rotational speeds and fluid resistances. We observed that the additional mass of the impeller is independent of rotational speed and fluid resistance, while the additional damping and stiffness are dependent only on rotational speed [12].

The equations of motion of the maglev impeller in the X direction, which are the same as in the Y direction, are as in Eq. (3).

$$\begin{aligned} &v_x = L\frac{di_x}{dt} + Ri_x + K_v\dot{x} \\ &(M+M_f)\ddot{x} + (C+C_f(\omega))\dot{x} + (K_x+K_{xf}(\omega))x - F_{dx} = K_i i_x. \end{aligned} \tag{3}$$

L and R are the inductance and the resistance of the coil respectively, K_v is the back electromotive force factor, K_i is the force–current factor, M is the impeller mass, C is the damping, and K_x is the negative stiffness.

The equations of motion in Eq. (3) were converted to the state space form as in Eq. (4). Based on Eq. (4) and the experimentally identified parameters, a reduced order observer, Eq. (5), as described by Luenberger [19], was designed for each rotational speed to estimate the disturbance force.

$$\begin{aligned} \dot{X} &= A_{11}X + A_{12}Y + B_1 v_x \\ \dot{Y} &= A_{21}X + A_{22}Y + B_2 v_x \end{aligned} \tag{4}$$

where $X = \begin{pmatrix} x \\ i_x \end{pmatrix}$, $Y = \begin{pmatrix} \dot{x} \\ F_{dx} \end{pmatrix}$, $B_1 = \begin{bmatrix} 0 \\ 1/L \end{bmatrix}$, $B_2 = \begin{bmatrix} 0 \\ 0 \end{bmatrix}$, $A_{11} = \begin{bmatrix} 0 & 0 \\ 0 & -R/L \end{bmatrix}$, $A_{12} = \begin{bmatrix} 1 & 0 \\ -K_v/L & 0 \end{bmatrix}$, $A_{21} = \begin{bmatrix} \frac{-(K_x+K_{xf}(\omega))}{M+M_f} & \frac{K_i}{M+M_f} \\ 0 & 0 \end{bmatrix}$, $A_{22} = \begin{bmatrix} \frac{-(C+C_f(\omega))}{M+M_f} & \frac{1}{M+M_f} \\ 0 & 0 \end{bmatrix}$.

The variation of the disturbance force was assumed to be zero ($\dot{F}_{dx} = 0$) because usually the estimation velocity is faster than the disturbance variation [12].

$$\dot{\hat{Y}} = A_{21}X + A_{22}\hat{Y} + B_2 v_x + G(\dot{X} - A_{11}X - A_{12}\hat{Y} - B_1 v_x) \tag{5}$$

where $\hat{Y}$ is the estimation of Y and $G = \begin{bmatrix} G_{11} & G_{12} \\ G_{21} & G_{22} \end{bmatrix}$ is the gain of the error term $(\dot{X} - A_{11}X - A_{12}\hat{Y} - B_1 v_x)$.

The disturbance force observer uses the displacement of the impeller (x), the current (i_x), and the applied voltage (v_x) in the coil to estimate the disturbance force ($\hat{F}_{dx}$). The same process is applied in the Y direction. In this paper the 'hat' symbol is used to refer to the estimate of a particular variable.

Table 1 shows the values of the parameters, inputs and output of the reduced order observer for a rotational speed of 1700 rpm and a flow rate of 5 L/min, in the X direction.

Table 1
Values of the parameters, inputs and output of the reduced order observer for rotational speed of 1700 rpm and flow rate of 5 L/min, in X direction.

		Values
Parameters	L	1.7×10^{-3} H
	R	6.4 Ω
	K_v	4.3 Vs/m
	K_i	4.3 N/A
	$M + M_f$	0.28 Kg
	$C + C_f(\omega)$	25 Ns/m
	$K_x + K_{xf}(\omega)$	-4.015×10^4 N/m
Inputs	v_x	−0.025 V
	i_x	−0.22 A
	x	-5.06×10^{-6} m
Output	F_{dx}	0.72 N

2.3. Radial disturbance forces on a maglev impeller

The estimated radial disturbance forces ($\hat{F}_d$) consist of a magnetic unbalance pull ($\hat{F}_{mag}$) generated by the difference between the magnetic center and the geometric center of the impeller; a rotating unbalance force ($\hat{F}_{rot}$) caused by the difference between the rotational and inertial centers of the impeller; the weight of the impeller ($\hat{F}_w$) when the pump is used in a non-horizontal position; a fluid-induced rotordynamic force ($\hat{F}_{rdf}$) caused by the wedge effect in the small gaps between the rotating impeller and the housing (as in hydrodynamic bearings); and a radial thrust ($\hat{F}_{rt}$) caused by the reaction to the pump flow. Since the radial thrust is related to the

pump flow, we isolated the radial thrust from all the disturbance forces.

This process consists of estimating the disturbance forces with the outlet of the pump open ($\hat{F}_{d\_open}$), and totally closed ($\hat{F}_{d\_closed}$). Since there is no generation of radial thrust ($\hat{F}_{rt}$) without pump flow, $\hat{F}_{d\_closed}$ would comprise of all the disturbance forces except the radial thrust. So it is possible to obtain the radial thrust by subtracting $\hat{F}_{d\_closed}$ from $\hat{F}_{d\_open}$, as shown in Eq. (6).

$$\begin{aligned}\hat{F}_{d\_open} &= \hat{F}_{mag} + \hat{F}_{rot} + \hat{F}_{w} + \hat{F}_{rdf} + \hat{F}_{rt}\\ \hat{F}_{d\_closed} &= \hat{F}_{mag} + \hat{F}_{rot} + \hat{F}_{w} + \hat{F}_{rdf}\\ \hat{F}_{rt} &= \hat{F}_{d\_open} - \hat{F}_{d\_closed}.\end{aligned} \tag{6}$$

3. Experimental setup

3.1. Maglev CBP

The two degrees-of-freedom radial controlled MB system is composed of two pairs of electromagnets located in the stator and a sandwich of two iron rings and a permanent magnet (PM) ring embedded in the rotor, as shown in Fig. 1(b). The PM ring provides closed magnetic circuits between the rotor and the electromagnets. In this way, the axial and angular motions are passively supported. Motion in the radial X and Y directions is controlled independently by the electromagnets [11,20].

The impeller is 51 mm in diameter, has six 5.5 mm high vanes, and is driven by a brushless DC motor located at the center of the CBP. The motor stator is comprised of twelve teeth and has a three-phase winding, and the motor rotor consists of an eight-pole Halbach PM array embedded in the impeller [20].

The CBP has an outer lateral fluid gap of 0.25 mm between the impeller and the lateral surface of the bottom housing of the electromagnets, an inner lateral fluid gap of 0.5 mm between the impeller and the lateral surface of the bottom housing of the motor, and all of the axial fluid gaps are 1 mm.

3.2. Relationship between pump continuous flow rate and radial thrust

First, the relationship between the flow rate and the radial thrust was identified under non-pulsatile conditions, estimating the radial thrust using disturbance force observers and measuring the flow rate using a conventional flow meter at the same time. Two pressure sensors (KL76, Nagano Keiki Co., Japan), with a measurement accuracy of 0.75 mmHg, at the inlet and outlet of the CBP were used to measure the differential pressure across it. An ultrasonic flow meter designed for medical uses (HT-320, Transonic System Inc., USA), located after the outlet pressure sensor, was used to measure the flow rate, which was altered by a screw clamp, located after the flow meter.

The ultrasonic flow meter used in this study has a measurement accuracy of 4%, a resolution of 50 mL/min and a bandwidth of 10 Hz. It is widely used in research involving blood pumps and flows in cardio–vascular systems [5,7,8]. Therefore, it was used as a reference to identify the relationship between the radial thrust and the flow rate.

The relationship was identified for rotational speeds of the CBP varying from 1300 to 1700 rpm in 100 rpm increments, which are the rotational speeds required to provide adequate blood flow to a recovered heart and to a failing heart, respectively, in our maglev CBP [14].

3.3. Mock circulatory loop with a pulsatile pump

After establishing the relationship between radial thrust and the non-pulsatile flow rate, this relationship was evaluated under pulsatile conditions, as in ventricular assistance. A mock circulatory loop with a pulsatile pump, as shown in Fig. 3, was built to simulate left ventricle assistance, as shown in Fig. 1(a).

The aorta simulator is an airtight tank with a volume of 5 L (area $=$ 100 $\times$ 100 mm^2, height $=$ 500 mm) which is used to simulate the compliance of the aorta. The left atrium simulator is an open reservoir. The cardiovascular resistances were simulated by altering a screw clamp located between the aorta simulator and the left atrium simulator. The left ventricle was simulated by a pulsatile pump (PP) with a latex diaphragm, driven by an air compressor and a vacuum pump, with two unidirectional valves simulating the aortic and the mitral valves.

The maglev CBP was connected to the mock circulatory loop, with the inlet receiving flow from the ventricle simulator, between two valves, and the outflow of CBP was united with the outflow of the PP, after the aortic valve. The same pressure sensors and ultrasonic flow meter described above were used to measure the differential pressure across the CBP and the pulsatile flow rate.

The mock circulatory loop was set to simulate a heart failing condition, before the connection of the ventricular assist device [14]. The beat frequency of the pulsatile pump was set to be 60, 70 and 80 bpm, and the maglev CBP was set to rotate from 1300 to 1700 rpm, in 100 rpm increments.

4. Experimental results and discussion

Positional changes of the geometric center of the maglev impeller may cause variations in the different types of radial disturbance forces inside the maglev CBP. In our experiment, we maintained the geometric center of the maglev impeller at the center of the pump, and no positional variation was observed with respect to the flow resistance. Furthermore, the amplitude of vibration of the maglev impeller was less than 20 μm, which is less than 8% of the fluid gap of 250 μm. Therefore, we assumed that the influence of the positional change of the maglev impeller on the magnitude of disturbance forces would be small and can be ignored.

4.1. Relationship between pump continuous flow rate and radial thrust

Fig. 4 shows the HQ curve of the maglev CBP at different rotational speeds in non-pulsatile conditions. We can see that the pump operating point (5 L/min, 100 mmHg) is achieved with a rotational speed of around 1700 rpm. At this point, the estimated radial thrust is 0.95 N. In Fig. 5 we can observe that an increase in the pump flow rate causes an increase in the absolute value of the radial thrust and that the rotational speed has little influence on the force direction, so only the absolute value of the radial thrust was used to estimate the flow rate. The influence of rotational speed on the force direction will be evaluated in the future work.

By using computational fluid dynamic (CFD) analysis to simulate the pressure distribution inside the pump, we observed that the pressure around -55 degrees is lower, so the variation of the direction of radial thrust is in this direction.

The relationship between the flow rate and the radial thrust is shown in Fig. 6. We observe a linear dependency of the flow rate on the radial thrust for each rotational speed. A single flow rate–force relationship, given by Eq. (7), relating the flow rate to the rotational speed and the radial thrust was obtained by a least squares method, as shown in Fig. 6.

$$Q_{\omega} = (12.53 - 0.0043\omega)\hat{F}_{rt}. \tag{7}$$

Our method is based on Eq. (1), proposed by Stepanoff, which relates the radial thrust to the head pressure and flow rate for

Please cite this article in press as: Pai CN, et al. Sensorless measurement of pulsatile flow rate using a disturbance force observer in a magnetically levitated centrifugal blood pump during ventricular assistance. Flow Measurement and Instrumentation (2009), doi:10.1016/j.flowmeasinst.2009.11.003

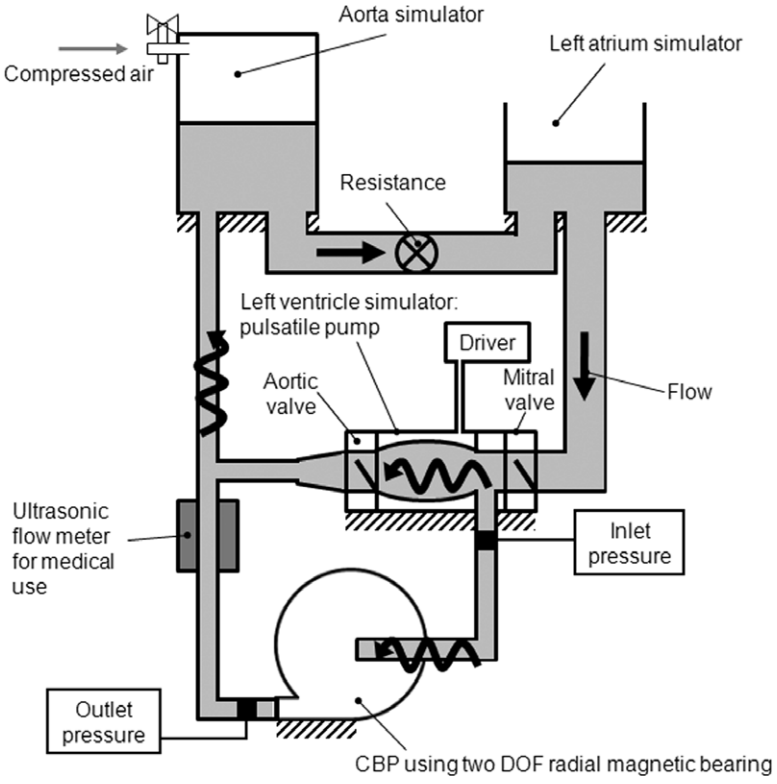

Fig. 3. Mock circulatory loop with a pulsatile pump.

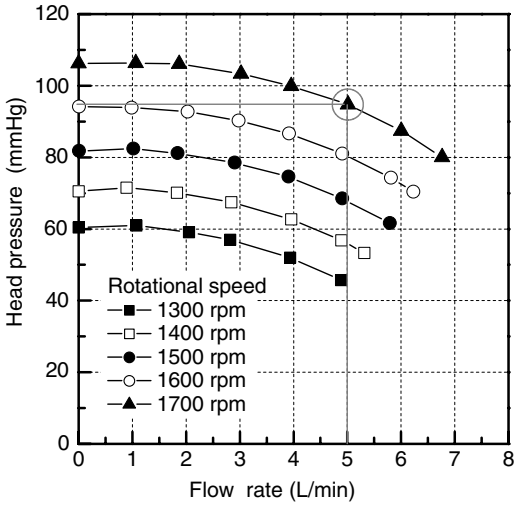

Fig. 4. Pump characteristic curve of the maglev centrifugal blood pump.

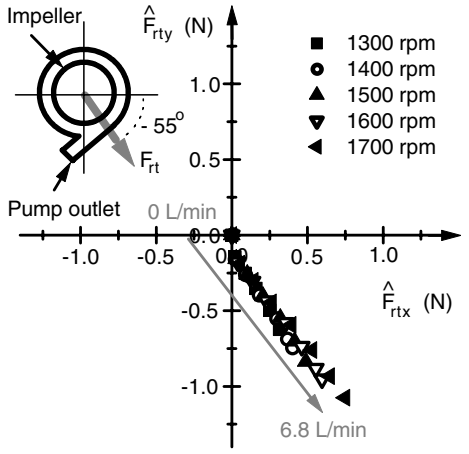

Fig. 5. Variation of radial thrust inside the pump with respect to rotational speed and flow rate.

centrifugal pumps. Eq. (1) does not contain a variable of rotational speed; however, the experimentally obtained flow rate–force relationship, Eq. (7), does contain a variable of the rotational speed. This is because the head pressure is a function of rotational speed and flow rate, and, assuming head pressure to be constant with respect to flow rate at a certain rotational speed, the variable for rotational speed was introduced in Eq. (7) to compensate for the actual variation of the head pressure.

The data shown in Fig. 6 are average values of real-time measurements of flow rate and estimations of radial thrust for 5 s, with a sampling frequency of 10 KHz. Since the standard deviation is 0.05 L/min, only the average value was plotted for each measurement.

Comparing Eq. (7) with Eq. (1) we can observe that it is possible to relate the bracketed term in Eq. (7), $(12.53 - 0.0043\,\omega)$, with certain dimensions of the pump and the head pressure. However, in order to increase the accuracy of the estimation, individual identification of the relationship for different maglev CBPs may be required.

4.2. The pulsatile flow rate estimation results

The pulsatile flow rate under different conditions was estimated by applying Eq. (7) with the estimated pulsatile radial thrust. Fig. 7 shows the comparison between the estimated and measured pulsatile flow rates with the CBP at 1300 and 1700 rpm and the pulsatile pump at 60, 70 and 80 bpm. The measured and estimated average pulsatile flow rate is shown at 1300 rpm and 60 bpm; while the measured and estimated amplitudes of pulsatile flow rate, defined as the peak-to-peak value, are shown at 1700 rpm and 60 bpm. The high correlation coefficient, $r > 0.94$,

Please cite this article in press as: Pai CN, et al. Sensorless measurement of pulsatile flow rate using a disturbance force observer in a magnetically levitated centrifugal blood pump during ventricular assistance. Flow Measurement and Instrumentation (2009), doi:10.1016/j.flowmeasinst.2009.11.003

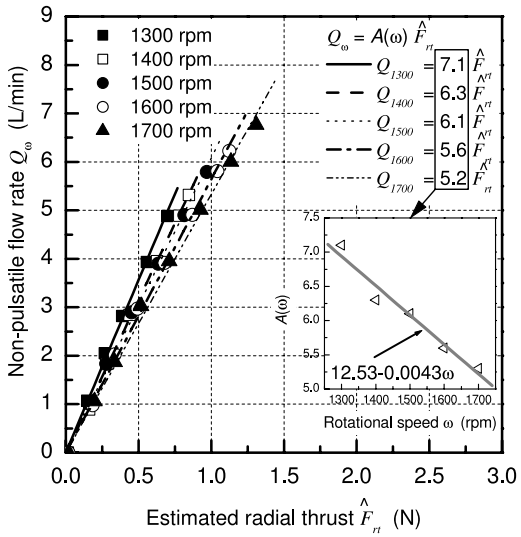

Fig. 6. Relationship between the non-pulsatile flow rate and the radial thrust.

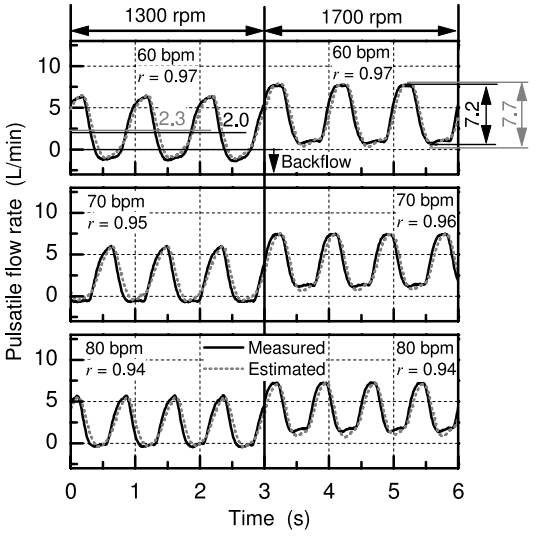

Fig. 7. Measured and estimated pulsatile flow rate at 1300 and 1700 rpm.

for all rotational speeds and beat frequencies, indicates a strong relationship between the estimated and measured values.

At 1300 rpm we also observe backflow caused by the low rotational speed of the CBP, an event that cannot be observed if only the average pulsatile flow rate is estimated. Backflow may cause blood stagnation inside the pump, leading to the formation of blood clots, and should be avoided.

From the results in Fig. 7, we can observe a delay between the measured and the estimated pulsatile flow rates. This delay is caused by the different cutting frequencies of the second-order low-pass filter (LPF) used in the ultrasonic flow meter (10 Hz) and in the disturbance force observer (3 Hz). A LPF of 10 Hz in the disturbance force observer is not sufficient to eliminate the vibration caused by the rotation of the impeller, and the estimated flow rate becomes too 'noisy'. Since the beating frequency of the natural heart is usually less than 1.5 Hz, we choose a LPF of 3 Hz for the disturbance force observer.

Changes in blood density and viscosity affect the processes for estimating pulsatile flow rate using motor power [7,8] and may also affect the estimation of the radial thrust. Ultimately this will also affect the pulsatile flow rate estimation method based on these parameters; therefore, further investigation is required.

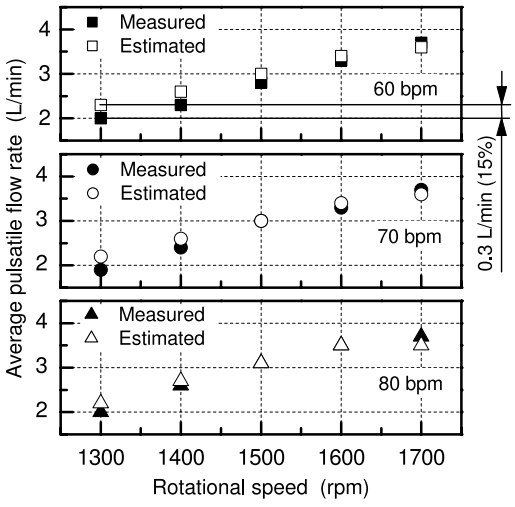

Fig. 8. Accuracy of the estimate of the average pulsatile flow rate.

In our method for estimating flow rate based on radial thrust, identification of the model parameters is required, which is the most complex part of this method. After estimating the radial thrust, estimating the flow rate becomes a very simple task. On the other hand, methods that estimate pulsatile flow rate using motor power require evaluation of the losses in the contact bearings, in the transmissions and in the motor for different rotational speeds and loads, and construction of such a database is also a complicated process.

4.2.1. Accuracy of estimate of average pulsatile flow rate

In this study, the flow rate as measured by the ultrasonic flow meter was considered as correct, and the process accuracy is defined relative to the measured value. Furthermore, the error is defined as the difference between the estimated and the measured flow rates.

Fig. 8 shows the errors in estimating the average pulsatile flow rates for all rotational speeds and beat frequencies. The maximum error is 0.3 L/min, which corresponds to 15% of the measured pump flow rate (2.0 L/min, at 60 bpm and 1300 rpm).

When using motor power in the flow rate estimation process, a CBP with a hydrodynamic bearing [5] showed an error of 0.3 L/min in estimating the average pulsatile flow rate for average flow rates in the range between 3.5 and 5.4 L/min, and another CBP with a magnetic bearing [6] showed an error of 0.5 L/min for flow rates in the range between 2.8 and 4.3 L/min. In CBPs with contact bearings, the estimation errors for average flow rates were 1.0 L/min for flow rates in the range between 2 and 6 L/min [7] and 1.9 L/min for flow rates in the range between 3 and 9 L/min [8].

Our results show average flow rate estimation errors up to 0.3 L/min for flow rates in the range between 1.9 and 3.7 L/min. This estimation accuracy is the same as the estimated value when using motor power in CBPs with non-contact bearings, and it is better than the values derived when using motor power in CBPs with contact bearings. The low estimation accuracy of CBPs with contact bearings is mainly caused by friction and the consequent wear of parts in contact, which increases the estimation error in long-term use.

4.2.2. Accuracy of estimate of amplitude of pulsatile flow rate

Fig. 9 shows the error in estimating the amplitude of pulsatile flow rate. The maximum error is 0.5 L/min, which corresponds to 7% of the measured amplitude pulsatile flow rate (7.2 L/min, at 60 bpm and 1700 rpm). A comparison with the estimation method of other groups using motor power could not be made because

Please cite this article in press as: Pai CN, et al. Sensorless measurement of pulsatile flow rate using a disturbance force observer in a magnetically levitated centrifugal blood pump during ventricular assistance. Flow Measurement and Instrumentation (2009), doi:10.1016/j.flowmeasinst.2009.11.003

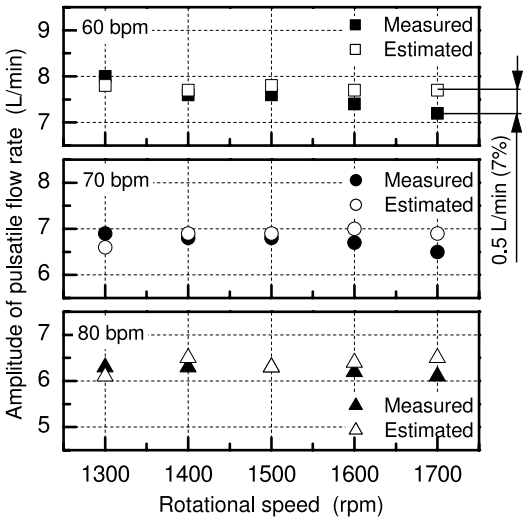

Fig. 9. Accuracy of the estimate of the amplitude of pulsatile flow rate.

the amplitude of the flow rate was not estimated for CBPs with non-contact bearings [5,6], and, although amplitudes of flow rate were estimated for CBPs with contact bearings [7,8], the accuracy of these was not given.

We can observe that the differences between the estimated and measured flow rates are within 15%, suggesting that our estimation method can substitute the use of an ultrasonic flow meter for the measurement of pump flow rate.

5. Conclusion

In order to measure the pulsatile flow rate through a maglev CBP during ventricular assistance, we developed a disturbance force observer to estimate the radial thrust. First, the relationship between radial thrust, flow rate and rotational speed under non-pulsatile conditions was obtained. This relationship was then evaluated under pulsatile conditions, and a high correlation coefficient ($r > 0.94$) was achieved between the measured and estimated pulsatile flow rates.

The maximum error in estimating the average flow rate is 0.3 L/min, which corresponds to 15% of the measured flow (2.0 L/min). The amplitude of the pulsatile flow rate was also estimated with a maximum error of 0.5 L/min, which corresponds to 7% of the measured amplitude of the pulsatile flow rate (7.2 L/min). Also, the occurrence of backflow can be observed.

In future work we plan to evaluate the influence of fluid density and viscosity on estimates of the radial thrust of the maglev impeller; to implement a method for estimating flow rate using motor power in our maglev CBP in order to compare the accuracy in estimating the pulsatile flow rate and the response speed; to evaluate the influence of variations in fluid density and viscosity on estimates of flow rate made by both methods; and to perform acute and chronic animal experiments in order to better evaluate the pulsatile flow rate estimation method.

Acknowledgement

This study was partly supported by Grants-in-Aid for Scientific Research no. 19360073 from the Japan Society for Promotion of Science and Electro-Mechanics Technology Advancing Foundation.

References

[1] Miller LW, Pagani FD, Russell SD, John R, Boyle AJ, Aaronson KD, Conte JV, Naka Y, Mancini D, Delgado RM, MacGillivray TE, Farrar DJ, Frazier OH. Use of a continuous-flow device in patients awaiting heart transplantation. N Engl J Med 2007;357:885–96.
[2] Rose EA, Gelijns AC, Moskowitz AJ, Heitjan DF, Stevenson LW, Dembitsky W, Long JW, Ascheim DD, Tierney AR, Levitan RG, Watson JT, Meier P. Long-term use of a left ventricular assist device for end-stage heart failure. N Engl J Med 2001;345:1435–43.
[3] Birks EJ, Tansley PD, Hardy J, George RS, Bowles CT, Burke M, Banner NR, Khaghani A, Yacoub MH. Left ventricular assist device and drug therapy for the reversal of heart failure. N Engl J Med 2006;355:1873–84.
[4] Dew MA, Kormos RL, Winowich S, Nastala CJ, Borovetz HS, Roth LH, Sanchez J, Griffith BP. Quality of life outcomes in left ventricular assist system inpatients and outpatients. ASAIO J 1999;45:218–25.
[5] Ayre PJ, Lovell NH, Woodard JC. Non-invasive flow estimation in an implantable rotary blood pump: A study considering non-pulsatile and pulsatile flows. Physiol Meas 2003;24:179–89.
[6] Tsukiya T, Akamatsu T, Nishimura K, Yamada T, Nakazeki T. Use of motor current in flow rate measurement for the magnetically suspended centrifugal blood pump. Artif Organs 1997;21:396–401.
[7] Tsukiya T, Taenaka Y, Nishinaka T, Oshikawa M, Ohnishi H, Tatsumi E, Takano H, Konishi Y, Ito K, Shimada M. Application of indirect flow rate measurement using motor driving signals to a centrifugal blood pump with an integrated motor. Artif Organs 2001;25:692–6.
[8] Ogawa D, Yoshizawa M, Tanaka A, Abe KI, Olegario P, Motomura T, Okubo H, Oda T, Okahisa T, Igo SR, Nose Y. Indirect flow rate estimation of the NEDO PI Gyro pump for chronic BVAD experiments. ASAIO J 2006;52:266–71.
[9] Hoshi H, Asama J, Hara C, Hijikata W, Shinshi T, Shimokohbe A, Takatani S. Detection of left ventricle function from a magnetically levitated impeller behavior. Artif Organs 2006;30:377–83.
[10] Masuzawa T, Kita T, Okada Y. An ultradurable and compact rotary blood pump with a magnetically suspended impeller in the radial direction. Artif Organs 2001;25:395–9.
[11] Pai CN, Shinshi T, Asama J, Takatani S, Shimokohbe A. Development of a compact maglev centrifugal blood pump enclosed in a titanium housing. J Adv Mech Des, Syst Manuf 2008;2:343–55.
[12] Pai CN, Shinshi T, Shimokohbe A. Estimation of the radial force using a disturbance force observer for a magnetically levitated centrifugal blood pump. J Eng Med [in press].
[13] Stepanoff AJ. In: Stepanoff AJ, editor. Centrifugal and axial flow pumps. 2nd ed. Florida: Krieger Publishing Company; 1957.
[14] Asama J, Shinshi T, Hoshi H, Takatani S, Shimokohbe A. Dynamic characteristics of a magnetically levitated impeller in a centrifugal blood pump. Artif Organs 2007;31:301–11.
[15] Fung YC. In: Fung YC, editor. Biomechanics—Mechanical properties of living tissues. 2nd ed. New York: Springer-Verlag Inc; 1993.
[16] Kim S, Cho YI, Hogenauer WN, Kensey KR. A method of isolating surface tension and yield stress effects in a U-shaped scanning capillary-tube viscometer using a Casson model. J Non-Newtonian Fluid Mechan 2002;103:205–19.
[17] Hinghofer-Szalkay H, Greenleaf JE. Continuous monitoring of blood volume changes in humans. J Appl Physiol 1987;63:1003–7.
[18] Sinnott RK. In: Sinnott RK, editor. Coulson & Richardson's chemical engineering. 4th ed. Chemical engineering design, vol. 6. Oxford (UK): Butterworth-Heinemann; 2005.
[19] Luenberger DG. An introduction to observers. IEEE Trans Autom Control 1971; ac-16:596–602.
[20] Asama J, Shinshi T, Hoshi H, Takatani S, Shimokohbe A. A compact highly efficient and low hemolytic centrifugal blood pump with a magnetically levitated impeller. Artif Organs 2006;30:160–7.

Please cite this article in press as: Pai CN, et al. Sensorless measurement of pulsatile flow rate using a disturbance force observer in a magnetically levitated centrifugal blood pump during ventricular assistance. Flow Measurement and Instrumentation (2009), doi:10.1016/j.flowmeasinst.2009.11.003